2011 International Nuclear Atlantic Conference - INAC 2011
Belo Horizonte, BH, Brazil, October 24 to 28, 2011
ASSOCIAÇÃO BRASILEIRA DE ENERGIA NUCLEAR - ABEN
ISBN: **978-85-99141-03-8**

USE OF THE MCNP-5C CODE FOR STUDY OF THE PDD CURVE AND ENERGY SPECTRUM BEHAVIOR IN FUNCTION OF THE ANODE INCLINATION ANGLE VARIATION IN LOW ENERGY X-RAY EQUIPMENT

Marco A. R. Fernandes[1], Victor A. B. Ribeiro[2], Rodrigo S. S. Viana[3] and Talita S. Coelho[3]

[1] Faculdade de Medicina de Botucatu, FMB.
Universidade Estadual Paulista "Júlio de Mesquita Filho"
Distrito de Rubião Jr., s/nº
18618-970 Botucatu – SP, Brazil.
marco@cetea.com.br / marfernandes@fmb.unesp.br

[2] Instituto de Biociências de Botucatu, IBB.
Universidade Estadual Paulista "Júlio de Mesquita Filho"
Distrito de Rubião Jr., s/nº
18618-970 Botucatu – SP, Brazil.
victor_abr@ymail.com

[3] Instituto de Pesquisas Energéticas e Nucleares (IPEN / CNEN – SP).
Av. Professor Lineu Prestes, 2242
05508-000, São Paulo – SP, Brazil.

ABSTRACT

This paper presents results of accomplished calculations with the MCNP-5C code to analyze the variation of the energy spectrum and PDD curves according with the anode inclination angle of the 50 kVp X-ray tube used in superficial radiotherapy. It intends to find the anode inclination angle, information not available at the manufacturer's catalog, and so, to model with more safely the radiation spectrum needed to obtain the PDD curve. The X-ray spectrum and the PDD curve are designed to three different anode angles: 20, 25 and 30º .The three PDD curves showed similar behaviors as a function of attenuation, it was not observed any systematic tendency of PDD alteration in function of the anode inclination. The PDD curve that presented closer values to the provided by the manufacturer is the ones obtained with 30º of anode inclination. The energy spectra showed similar behavior of the emitted radiation intensity (photons/cm^2) in function of the energy (keV) for the three target angulation. All three spectra exists an energy peak of 11.67 keV, which may be involved with the L-shell characteristic radiation of the tungsten element. The not filtered energy spectrum for 30º of anode angulation was created to better evaluate the found characteristic radiation peak, and it showed two energy peaks at 9.248 and 11.673 keV, also due possibly to the L-shell characteristic radiation of the tungsten. Though more refined studies of the obtained results at this work are necessary; the MCNP-5C code showed to be appropriate for analyzing of attenuation curves of the superficial radiotherapy beams.

2011 International Nuclear Atlantic Conference - INAC 2011
Belo Horizonte, BH, Brazil, October 24 to 28, 2011
ASSOCIAÇÃO BRASILEIRA DE ENERGIA NUCLEAR - ABEN
***ISBN:* 978-85-99141-03-8**

1. INTRODUCTION

Tumors are caused by the uncontrolled growth of cells, giving rise a new tissue, the neoplasm. The skin tumors are responsible for about 25% of all diagnosed neoplasms. The most common are cell basal carcinoma (CBC) and cell squamous carcinoma (CSC) and the melanomas. The CSC's and the CBC's are radiosensitive and can be to send to radiotherapy.

Before the widespread diffusion of linear accelerators with electron beams, the treatment of these lesions was, and in some places still is, accomplished through superficial radiotherapy equipments with X radiation, as the Dermopan2® equipment of Siemens brand, operating at the Radiology service of the UNESP Veterinary Hospital of Araçatuba, with maximum energy of 50 kVp. The lack of greater knowledge of the energy spectrum from this equipment limits the routines of radiotherapy services to the simple use of radiometric parameters provided at the manufacturer’s catalog, without at least proceed to the validation with other dosimetric system, what can compromise the dosimetric calculations quality determined by the medical physicist, often imbued of uncertainty.

It is worth emphasizing that recent technological developments have been providing modern radiotherapy equipments, such as the Intrabeam® that performing procedures of intra-operative radiotherapy with 50 kVp X-ray beams.

Therefore, it is a lot important the study of computing systems with calculation methods and algorithms dedicated to the routine of the radiotherapy physic.

The percentage depth dose (PDD) curve is a radiometric parameter of the radiation beams used at radiotherapy, and it must be obtained at the commissioning of the treatment machines. In the dosimetry procedures of clinical beams, the PDD values are measured with ionization chambers suitable for the considered energies, doing the scanning of the radiation field inside a water simulator (phantom), or acrylic attenuators, or solid water. The measured PDD curves are compared with documents provided by the manufacturer, however, it doesn’t have further details of the beam energy spectrum.

With a constant development of computer systems and a better understanding of the calculation algorithms, the Monte Carlo Method has been demonstrating to be an important tool for studies of the radiometric parameters of clinical beams, and it already is added to the routines of the systems used by several manufacturers of specialized software. It also demonstrates as powerful tool for simulations of relevant problems at the radiation dosimetry. In this work it were developed simulations with the Monte Carlo Method, MCNP-5C code, for a more accurate modeling of the radiation spectrum needed for achievement of the PDD curve.

We desire to develop geometric modeling and computer simulations with the MCNP-5C code to discover the characteristic of an X-ray tube not provided at the manual and necessary for obtaining the 50 kVp energy spectrum from a superficial radiotherapy equipment of the Siemens brand, Dermopan2® model.

2011 International Nuclear Atlantic Conference - INAC 2011
Belo Horizonte, BH, Brazil, October 24 to 28, 2011
ASSOCIAÇÃO BRASILEIRA DE ENERGIA NUCLEAR - ABEN
ISBN: 978-85-99141-03-8

2. MATERIALS AND METHODS

The Dermopan2® model superficial radiotherapy equipment (Figure 1 and 2) was used to study the radiation spectrum emitted from the equipment and its behavior when interacting with the biological tissue (phantom).

Figure 1. Dermopan2®

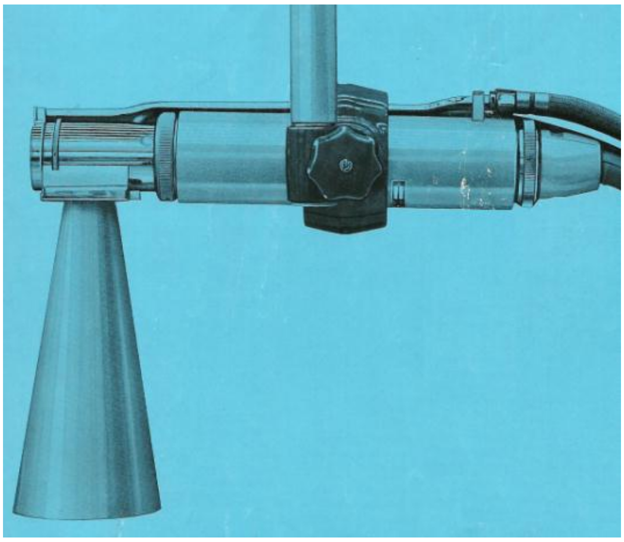

Figure 2. Dermopan2®

Figure 3 was taken from the manual for beam dosimetry; the graph represents the measured percentage depth dose (PDD) for 29 kVp (2), 43 kVp (3) and 50 kVp (4) energy, and using the Locator with a diameter of 4 cm (size of the radiation field). From the Figure 3, it was possible to build the same curves at the Origin program (Figure 4), useful for later comparison with the simulated PDD curves.

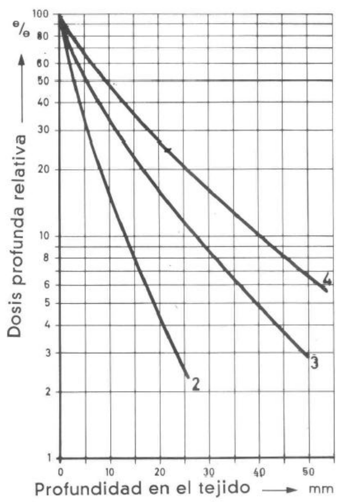

Figure 3. PDD (manual)

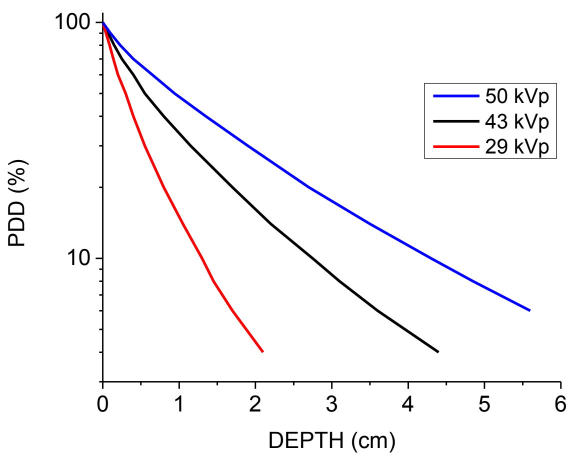

Figure 4. PDD (manual) built at the Origin program

ISBN: **978-85-99141-03-8**

For the simulations of the studied beam behavior (50 keV) it was used the Monte Carlo Method (MCM) with the MCNP-5C code. This is a statistical method used in stochastic simulations; involves the generation of observations, through various experiments, some probability distributions and the use of obtained samples to approximate the interest function. The MCNP-5C code is a recognized internationally code for analysis of neutrons, gamma rays and electrons transport by the Monte Carlo Method.

The characteristics of the X-ray tube provided in the Dermopan2® equipment manual were used for geometric construction of the radiation source. Computer simulations were performed considering the composition of the X-ray tube target being of tungsten ($^{184}W_{74}$), the beam inherent filtration being of beryllium ($^{9}Be_{4}$) (1 mm) and about 2.1 cm from the target, the head shield being of lead ($^{207}Pb_{82}$), the additional filter of aluminum ($^{27}Al_{13}$), about 3.5 cm from the anode, the size of the focal point (focal area) of the electron beam has 6.5 mm in diameter, application of the plumbiferous glass locator with source-surface distance (SSD) of 30 cm and radiation field with 4 cm in diameter, all these data were reported at the equipment catalog and the filtration-target distances were taken from Figure 5, also available in the manual.

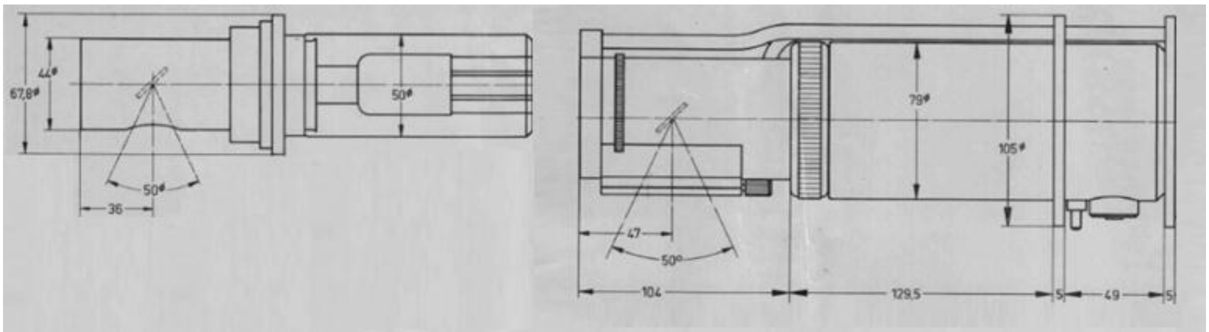

Figure 5. Illustration inside of the Dermopan2® equipment

Figure 6 illustrates the geometric construction of the Dermopan2® head (made at the program's input), adopting a 1 mm additional filter of thick. It was possible to extract from the simulations the 50 kVp radiation spectra – useful for analyzing the beam behavior – before and after the photons being filtered by aluminum.

For the sampling of the PDD curve, the plumbiferous glass Locator and the phantom were added at the geometry (Figure 7). As the SSD (source-surface distance) is 30 cm, the Locator must have 26.4 cm long, moreover 4 cm in diameter and, for the simulations, the 5 mm of the glass thick was replaced by 2 mm of lead, which is an equivalent approach. The Locator was placed just below the additional filter and in contact with the phantom, water – has a similar behavior to the biological tissue. Sixteen layers are specified within the phantom for calculating the PDD, being the first five with 1 mm of thick and the subsequent with 0.5 cm.

The PDD express as a percentage the absorbed dose at any depth *d* to the absorbed dose at a fixed reference depth *d0*, along the central axis of the beam; as it is showed in the formula 1.

2011 International Nuclear Atlantic Conference - INAC 2011
Belo Horizonte, BH, Brazil, October 24 to 28, 2011
ASSOCIAÇÃO BRASILEIRA DE ENERGIA NUCLEAR - ABEN
ISBN: 978-85-99141-03-8

$$PDD = \frac{D_d}{D_{d0}} \times 100 \qquad (1)$$

As it was not informed the tungsten anode inclination, it was required studies for 20º, 25º and 30º angles (since for radiotherapy equipment the target inclination is around from 20 to 30º), obtaining their energy spectra and PDD curves. The behavior of the simulated PDD curves was compared with the behavior of the provided at the manual curve and used in calculations for clinical planning; and thus, it was extracted the angle that provides more consistent values.

The focal point of the electron beam that collides with the tungsten anode, informed as being 6.5 mm, is discriminated through the MCNP-5C code determining the cross-sectional diameter of the electron beam, calculated at Figure 8.

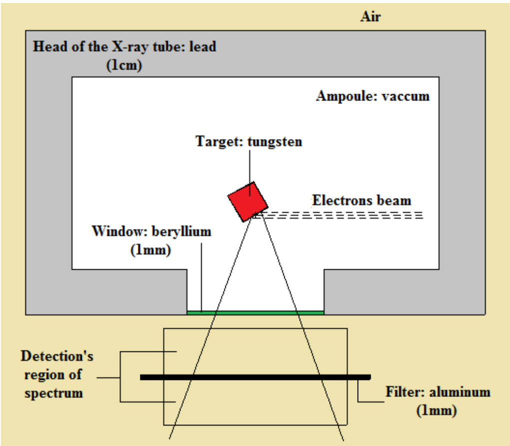

Figure 6. Head of the X-ray tube for the beam and spectrum simulation

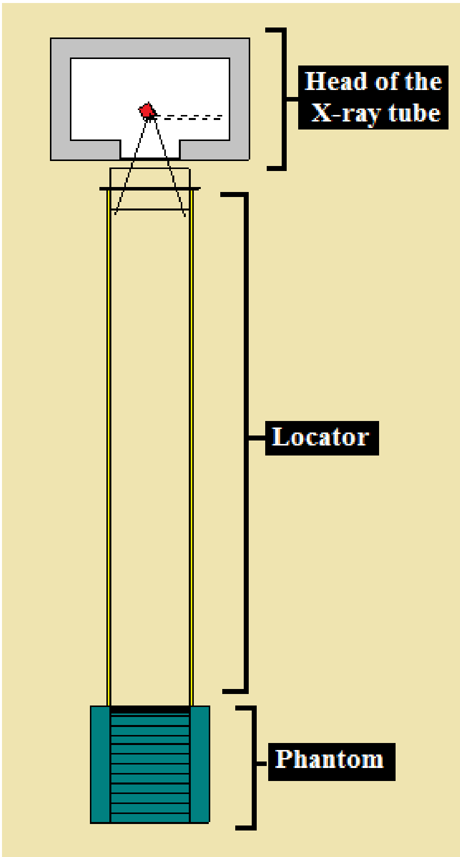

Figure 7. System for PDD simulation

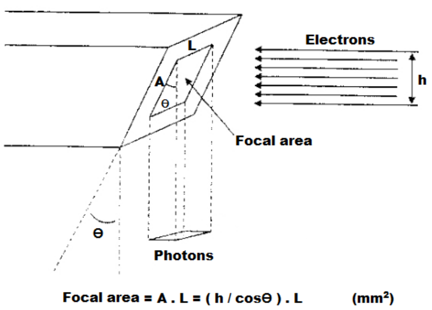

Figure 8. Focal area at X-ray ampoules

As the focal point has 6.5 mm in diameter, an area of 33.18 mm^2 ($A = \pi. R^2 = \pi. (3.25)^2$) is created. This area is equivalent for the circular area of a square of side 5.76 mm. Applying the formula at Figure 8 ($33.18 = (h / \cos(\theta)). 5.76$) and considering the different angles, it calculates the cross-sectional areas of the electron beam and, subsequently, the equivalent diameters to those areas for further simulation.

ISBN: **978-85-99141-03-8**

The generate radiation spectra by the simulations were qualitatively analyzed in comparison with the literature that predicts its specific behavior.

3. RESULTS AND DISCUSSION

For a correct simulation of the system, it was calculated the cross-sectional diameter of the circular electron beam colliding with the tungsten anode, being this diameter dependent of the anode inclination angle as seen at Table 1.

Table 1. Anode angle of the X-ray tube.

	Anode inclination		
	20º	25º	30º
h	5,41 mm	5,22 mm	4,99 mm
Diameter of the cross-sectional	6,30 mm	6,19 mm	6,05 mm

At Figure 9, there are the simulated PDD curves for the three adopted inclinations. Through their values it was able to compare with the PDD curve extracted from manual, and analyze witch inclination provides values closer to the desired.

The Table 2 presents more clearly the values of radiation attenuation for the three studied anode angles.

Table 2. PDD values for different anode inclinations.

PDD (%)	20º	25º	30º	Manual	Relative error (%)		
	Depth (cm)				E_I	E_{II}	E_{III}
100	0,00	0,00	0,00	0,00	0,0	0,0	0,0
90	0,095	0,113	0,115	0,10	5,0	13,0	15,0
80	0,203	0,290	0,242	0,23	11,7	26,1	5,2
70	0,416	0,415	0,443	0,40	4,0	3,8	10,8
60	0,700	0,698	0,651	0,65	7,7	7,4	0,2
50	1,125	1,017	0,987	0,94	19,7	8,2	5,0
40	1,639	1,407	1,430	1,35	21,4	4,2	5,9
30	2,100	1,957	1,944	1,90	10,5	3,0	2,3
20	2,933	2,967	2,742	2,70	8,6	9,9	1,6
14	3,784	3,730	3,451	3,50	8,1	6,6	1,4
10	4,530	4,510	4,337	4,30	5,3	4,9	0,9
8	4,800	4,910	4,639	4,85	1,0	1,2	4,4
6	5,160	5,570	5,510	5,60	7,9	0,5	1,6
		Mean relative error (%)			9,2	7,4	4,5

E_I: relative error between the PDD values with 20º of anode inclination (20º) and the values extracted from the manual (Manual). E_{II} e E_{III}: the same comparison, but for, respectively, 25º and 30º.

ISBN: 978-85-99141-03-8

The observation of the found relative error suggests that the better anode inclination angle of the X-ray tube is 30º (Figure 10).

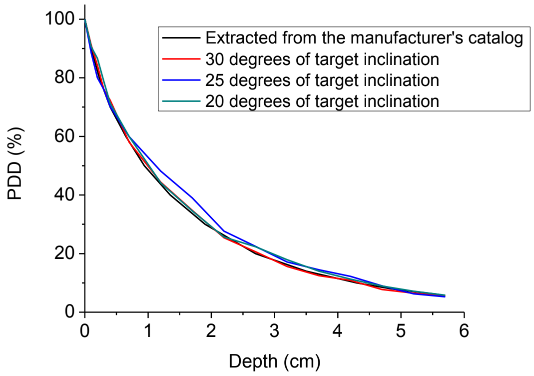

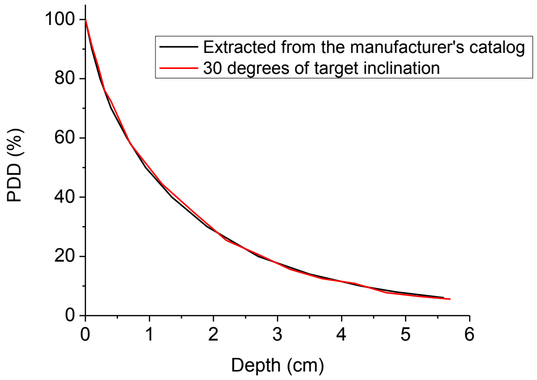

Figure 9. Simulated PDD curves

Figure 10. Simulated PDD curve – 30º

The Figure 11 shows the radiation spectra of 50 kVp – after being filtered by 1 mm of aluminum – obtained for the tree different target angulation; in the simulation were adopted 100 energy ranges between 1 and 50 keV. For analyzing the characteristic radiation peaks, it is interesting to plot the spectrum generates without the additional filtration (aluminum) (Figure 11), considering the more appropriated target inclination (30º).

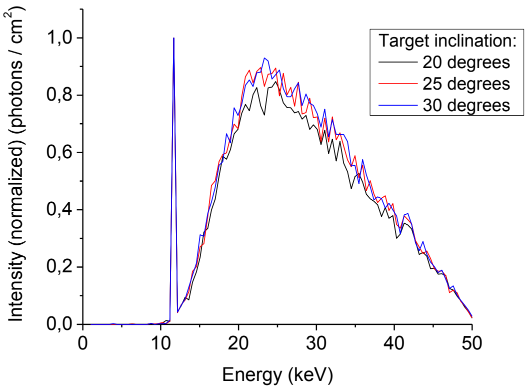

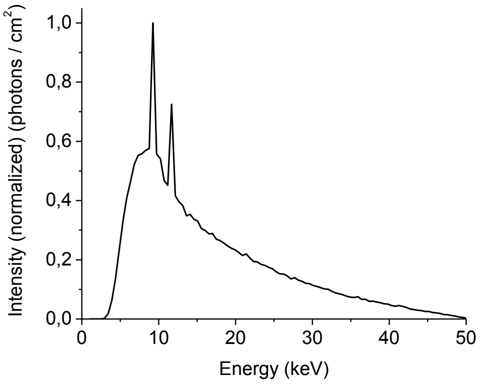

Figure 11. Simulated spectra – 50 kVp

Figure 12. Simulated spectrum – 50 kVp, without additional filtration

At the tree spectra (Figure 11), it exists a greater intensity peak, exactly with the same shape and energy of 11.67 keV; at the picture they are superimposed and evidence their independence to the target angulation.

2011 International Nuclear Atlantic Conference - INAC 2011
Belo Horizonte, BH, Brazil, October 24 to 28, 2011
ASSOCIAÇÃO BRASILEIRA DE ENERGIA NUCLEAR - ABEN
ISBN: 978-85-99141-03-8

The spectrum of the Figure 12 was collected in a region about 0.8 cm bellow the beryllium filter, so the beam didn’t suffer the filtration caused by the aluminum. Two evident peaks are revealed by the graph. The higher intensity peak has energy 9.248 keV and the lower intensity 11.673 keV. The Figure 13 shows an attenuation curve for the tungsten and aluminum.

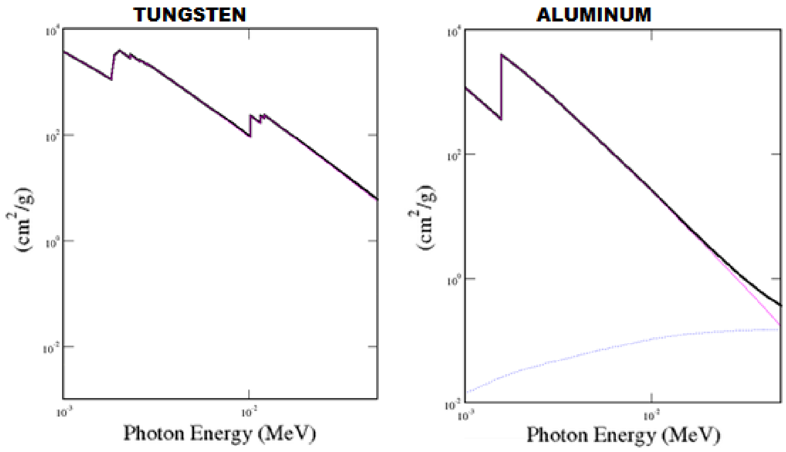

Figure 13. Photoelectric absorption (blue), Compton scattering (rose) and total attenuation (black) curves – Literature (NIST)

There are regions where occurs an increase on energy absorption by the orbital electron, resulting its ejection from the tungsten atom, this within the energetic limit from 1 to 50 keV. After the electron ejection, characteristic radiation is emitted, since a lower energy electron fills the shell with a less electron, releasing as characteristic radiation the energy difference between the orbitals. The low energy attenuation region, from 1 to 2 keV, results the emission of very low energy characteristic radiation, that is absorbed by the own walls of the X-ray tube. For the higher energy region, the attenuation values for each orbital shell are better quantified at the tables below (Table 3).

Table 3. Energy values for the L, M and N shell of the tungsten.

Shell	Energy (keV)
L_I	12.1
L_{II}	11.54
L_{III}	10.21

Shell	Energy (keV)
M_I	2.82
M_{II}	2.575
M_{III}	2.281
M_{IV}	1.872
M_V	1.809

Shell	Energy (keV)
N_I	0.589
N_{II}	0.485
N_{III}	0.418
N_{IV}	0.253
N_V	0.239
N_{VI}	0.031
N_{VII}	0.029

The energy values of the found peaks at the graph are not completely accurate. At the quantification of the 50 kVp spectrum we delimited energy ranges of 0.485 keV, so that the MCNP-5C code makes the photons count with energy within this limit (photons fluency).

ISBN: **978-85-99141-03-8**

Thus, the found energy values can vary from 8.763 to 9.248 keV, and from 11.188 to 11.673 keV; without account inherent variations of the own simulation.

From the quantum physics we know that there are transitions rules between orbital shells. Therefore, among the allowed transitions and the transitions that result photons with energy within the desired ranges, occur: $M_{II} – L_{II}$, $N_{IV} – L_{II}$, $N_I – L_I$, $N_{VI} – L_{II}$, $N_{VII} – L_{II}$, shell L_{II} and $N_{II} – L_I$; with respective energy of: 8.953, 11.286, 11.503, 11.505, 11.515, 11.539 and 11.610 keV. Besides other transitions with energy close to those found: $M_{IV} – L_{III}$, $M_V – L_{III}$, $M_{III} – L_{II}$, $M_{IV} – L_{II}$, $N_V – L_{III}$, $N_{III} – L_{II}$, $N_V – L_I$ and shell L_I; with respectively: 8.335, 8.398, 9.269, 9.673, 9.964, 11.121, 11.862 and 12.100 keV. Photons with energy a little higher than the found peaks may have been generated, but due to Compton scattering them energy were reduced. The transitions indicated above can explain the characteristic radiation peaks observed at the Figure 11 and 12.

4. CONCLUSIONS

The simulations of the PDD curves show similar behaviors in function of attenuation on the depth from 0.0 cm to 5.7 cm, with the higher difference between the values of about 9%, presented between the 20º simulated and extracted from the manual curves; it was not verified any systematic tendency of PDD alteration in function of the anode inclination.

With satisfactory results (4.5% of error), it was evident that the X-ray tube anode angulation of the Dermopan2® equipment is close to 30º.

The energy spectra show a similar behavior of the emitted radiation intensity (photons/cm^2) in function of the energy (keV) for the three analyzed target angulations. The higher photons intensity region is at the range from 20 keV to 35 keV. All three spectra present an energy peak on 11.65 keV, what it can be involved mainly with the characteristic radiation of the L shell of tungsten that makes up the target.

Known the anode inclination, it was built the not filtered radiation spectrum of 50 keV, which showed two peaks of characteristic radiation of the tungsten, also perfectly explained by the various transitions between shells that occur at the energy range from 9 and 11 keV.

Though more refined studies of the obtained results at this work are still necessary, it is possible point the MCNP-5C code as an appropriate procedure for analyzing of attenuation curves of the superficial radiotherapy beams.

ACKNOWLEDGMENTS

The authors thank the FAPESP for the financial support (process nº 2011/09756-5); the professionals of the Radiotherapy Service of the College of Medicine’s Hospital of Botucatu and Radiology and Small Animals’ Surgery Service of the UNESP Veterinary Hospital of Araçatuba for the availability of radiation equipments; the Nucleata Radiometria company of Araçatuba for the support at radiometric procedures; the researchers of the Nuclear

2011 International Nuclear Atlantic Conference - INAC 2011
Belo Horizonte, BH, Brazil, October 24 to 28, 2011
ASSOCIAÇÃO BRASILEIRA DE ENERGIA NUCLEAR - ABEN
ISBN: **978-85-99141-03-8**

Engineering Center (CEN) of the Nuclear and Energetic Research Institute (IPEN/CNEN-SP) for supply and technical support with the MCNP-5C code.

REFERENCES

BRIESMEISTER, J.F. **MCNP: A General Monte Carlo N-Particle Transport Code**, version 5C. LA-13709-M. Los Alamos: Los Alamos Scientific Laboratory, 2000. 484p.

CURRY, T.S.; DOWDEY, J.E.; MURRY, R.C. **Christensen's Physics of Diagnostic Radiology**. Philadelphia: Lippincott Williams & Wilkins, 1990. 431p.

KHAN, F.M. **The Physics of Radiation Therapy**. Philadelphia: Lippincott Williams & Wilkins, 2003. 560p.

FERNANDES, M.A.R. ***Utilização de moldes radioativos especiais de folhas de Ouro-198 no tratamento de tumores de pele***. 2000. 170f. Doctoral dissertation – Instituto de Pesquisas Energéticas e Nucleares (IPEN/CNEN-SP), São Paulo. 2000.

BERGER, M.J.; COURSEY, J.S.; ZUCKER, M.A.; CHANG, J. **Stopping-Power and Range Tables for Electrons e X-Ray Transition Energies.** NIST – Physics Laboratory. Available at: <http://www.nist.gov/pml/data/index.cfm>. Accessed: June 20, 2011.